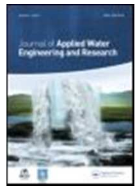

Simulation of river water temperatures during various hydro-peaking regimes

Journal:	*Journal of Applied Water Engineering and Research*
Manuscript ID	TJAW-2015-0031.R1
Manuscript Type:	Research Paper
Date Submitted by the Author:	n/a
Complete List of Authors:	Bakken, Tor; Norwegian University of Science and Technology, Department of Hydraulic and Environmental Engineering King, Tyler; Norwegian University of Science and Technology, Department of Hydraulic and Environmental Engineering Alfredsen, Knut; Norwegian University of Science and Technology, Department of Hydraulic and Environmental Engineering
Keywords:	Eco-hydraulics, Hydroinformatics, River hydraulics, Water temperatures, Day degree, hydro-peaking, thermo-peaking

Simulation of river water temperatures during various hydro-peaking regimes

Simulation of river water temperatures during various hydro-peaking regimes

Authors
Tor Haakon Bakken[1 & 2] (corresponding author), Tyler King[3] & Knut Alfredsen[2]

[1] SINTEF Energy Research, Sem Sælands vei 11, NO-7465 Trondheim, Norway. E-mail: tor.haakon.bakken@sintef.no. Tlp: +47 95156944.

[2] Norwegian University of Science and Technology (NTNU), Department of Hydraulic and Environmental Engineering, Norway.

[3] University of New Hampshire, US / visiting researcher Norwegian University of Technology and Science (NTNU)

Abstract
Hydro-peaking is a type of hydropower operations characterized by rapid and frequent changes in flow, possibly also leading to similar changes in water temperatures ('thermo-peaking'). This study examines water temperature variations and caused by the present hydro-peaking regime in Nidelva River (Norway), and the impacts future changes in the operation of the hydropower system might introduce.

The simulated future scenarios indicate that only limited changes are expected to happen compared to the present situation, measured as changes in accumulated degree-days. The model simulations predict a reduction in the range of 50 degree-days for two of the scenarios and an increase in approximately 40 degree-days for the third scenario. These results are further transformed into changes in salmon egg development and time of hatching, which corresponds to a few days delay in hatching in all three scenarios, and also a slight delay in swim-up for two of the three scenarios.

Keywords: water temperatures, hydro-peaking, thermo-peaking, degree-day

1 Introduction

Climate change and the needs for reductions in the use of fossil fuels call for the development of renewable energy sources. Sources such as solar and wind power are non-regulated sources, as they produce electricity only in periods with favourable weather conditions. In order to secure sufficient and stable supply of electricity to the consumers, the need for regulating energy production will increase. The outcome of such a change in the energy mix with a larger share on non-regulated sources would be a larger need for regulated services, which reservoirs and pumped-storage hydropower can provide (Gabrielsen & Grue 2012; IPCC 2011).

Regulation of river basins for hydropower generation introduces changes to the natural hydrological system (Maddock et al. 2013). While run-of-river hydropower plants cause small changes to the natural flow regime due to its limited storage capabilities, reservoir-based hydropower can change the natural hydrological system dramatically (IPCC 2011). Hydro-peaking is a variant of hydropower production, characterised by introducing rapid and frequent changes in discharge through a hydropower plant. The term 'hydro-peaking' is, however, broad and vaguely defined in the literature, and other terms are also found describing the same phenomenon, such as intermittent hydropower generation (Moog 1993), hydropower peaking (Valentin et al. 1995), rapid flow decreases (Bradford 1997), sudden flow variations (Liebig et al. 1999), fluctuating flow (Vehanen et al. 2000), rapid changes in flow (Saltveit et al. 2001), pulse power generation (Scruton et al. 2003) and peaking flows (Berland et al. 2004). Hydro-peaking has been used to describe both the operational pattern of hydropower plants (e.g. pulse power generation) and the flow variations in rivers downstream the power plant outlets (e.g. rapid flow decreases) (Sauterleute & Charmasson 2014). Tools are now available to calculate hydro-peaking parameters based on timeseries of discharge and water level (Sauterleute & Charmasson 2014; Carolli et al. 2015; Greimel et al. 2016).

River water temperature has increasing interests as a topic of research as greater understanding of its importance for ecosystem functions is recognized (Caissie 2006). Water temperature has been identified as a primary factor in the presence, productivity, and metabolism of riverine microorganisms, invertebrates, and fish populations (Ward & Stanford 1979; Vinson 2001; Schlosser et al. 2000) and the health of the ecosystem and the inhabited organisms is determined by specific temperature ranges of the ambient water (Coutant 1999). Deviations from these ranges can disrupt life cycles, create ecosystem imbalance and, eventually, ecosystem collapse (Ward & Stanford 1979). Because of the sensitive relationships between temperature and biological processes, it is of utmost importance to understand the changes in water temperature introduced by human intervention to the river systems, and its impact on the aquatic ecosystem. Hydro-peaking may cause similar rapid and frequent changes to the water temperature, known as thermo-peaking (Toffolon et al. 2010). Zolezzi et al. (2011) have derived methods for identifying thermo-peaking events, while Steel & Lange (2007) have described the scale, variability, and recurrence of thermo-peaking. The ecological responses to rapid changes in water temperature are, however, not thoroughly studied and understood, with exceptions such as Bruno et al. (2013) that studied the effect on the benthic community.

The purpose of the case study of Nidelva River in mid-Norway study has been to:

- Document and analyze the changes in water temperature introduced by hydro-peaking ('thermo-peaking').
- Demonstrate the capability of a hydraulic tool to simulate rapid changes in flow and river water temperatures caused by hydro-peaking under the current operational regime ('base-line').
- Define and simulate possible future scenarios for hydro-peaking introduced by large-scale development of non-regulated energy sources (i.e. wind power) and its impact on water temperatures.
- Demonstrate how the impacts on salmon egg development and ice production introduced by changes in the operational regime can be assessed, based on the water temperature simulations.

Nidelva River downstream of the outlet of Bratsberg and Leirfossen power plants is a highly productive salmon river, producing 4-10 tons annually. It is also a spawning ground for

Atlantic salmon (*Salmo salar*) and sea trout (*Salmon trutta*) - two species known to be sensitive to alterations in river temperature (Johnsen et al. 2010; Hvidsten 1985; Berland et al. 2004). Nidelva is of great importance to the local community and holds numerous stakeholders in the forms of recreational fishermen, paddle sport enthusiasts, the local hydropower company, and the 180 000 inhabitants of Trondheim (Fremstad & Thingstad 2007).

2 Study site, tools applied and calibration perfomance

2.1 Study site Nidelva River in mid-Norway

The Nea-Nidelva watershed is located in Sør-Trøndelag County in mid-Norway (Figure 2.1). The total area of the watershed is 3118 km^2 and the average annual discharge is approximately 90 m^3/s at the outlet to the Trondheim Fjord. The watershed includes a series of 17 hydropower plants producing an annual average of 2550 GWh. Selbusjøen reservoir, with a surface area of 58 km^2, is the final reservoir in the ladder of hydropower production facilities in the Nea-Nidelva watershed.

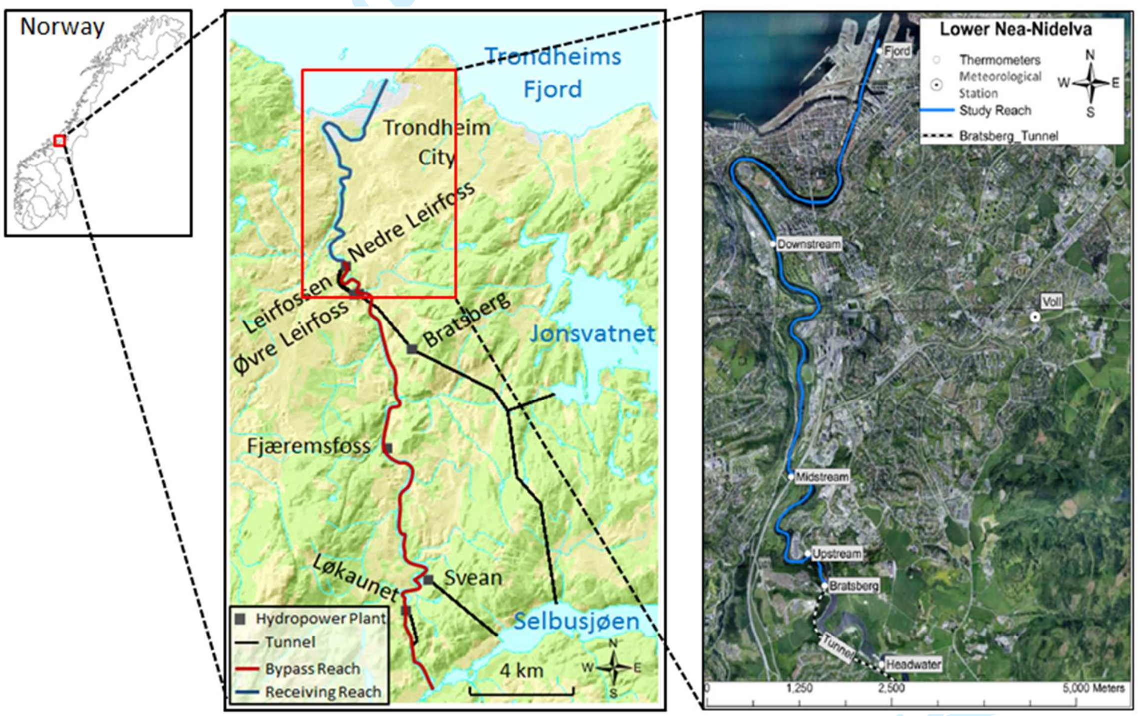

Figure 2.1. Right: Study reach between points labelled 'Upstream' and 'Downstream' (adapted from Google Earth). Center: Lower Nea-Nidelva watershed. Left: Case study location in Norway.

There are two hydrologic pathways from Selbusjøen to the study reach; through 16 kilometers of tunnel through the Bratsberg hydroelectric power plant, or as surface flow along an 18 kilometer long bypass reach (Figure 2.2). Water that flows down the bypass reach encounters a series of run-of-river hydropower stations. There are two hydropower facilities located just upstream of the study reach that are developed around two natural water falls: Øvre and Nedre Leirfossen (Ø.L. and N.L. in Figure 2.2, respectively). Historically, these falls fed two different hydropower plants, but in recent developments, a newer subterranean station now spans both water falls taking water from upstream of Øvre Leirfoss directly to the bottom of Nedre Leirfoss, forming a confluence with the outlet from Bratsberg in Nidelva River. This confluence is the upstream boundary of our study reach, approximately 10 km upstream of Trondheim Fjord.

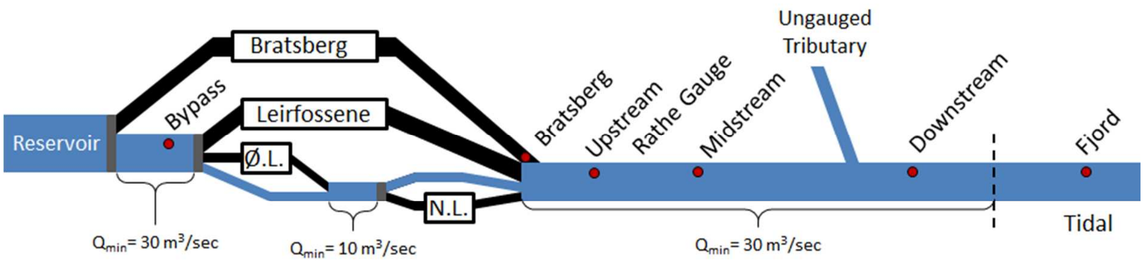

Figure 2.2. Pathways of the water from Selbusjøen reservoir into the study reach, starting at Bratsberg and ending where the interference with the tidal water starts.

The Bratsberg hydroelectric power plant makes use of two identical turbines with a maximum operational discharge of approximately 100 m^3/s (OED 2006), while the new Leirfossen hydroelectric power plant has two turbines with discharge capacities of 30 and 55 m^3/s (Engebrethsen 2010). The hydropower production in Nidelva can be considered hydro-peaking as it is causes rapid and frequent flow variations on top of the minimum flow requirement of 30 m^3/s (OED 2006). The present hydro-peaking operations in Nidelva are mild to moderate with respect to flow/peaking ratio, but the frequency in change in flow is high compared to other rivers in Norway and Austria (Bakken et al. 2012). The maximum flow/peaking ratio (maximum discharge divided by minimum discharge) is 6:1, as the maximum production capacity through Bratsberg and Leirfossen power plants is 180 m^3/s. The frequency is typically be 1-2 peaking events per day (Bakken et al. 2012).

Selbusjøen reservoir is regulated to maintain a water surface elevation between 151.9 and 158.2 meters above sea level, and the Bratsberg intake is placed within the top 6.3 meters of the reservoir year round (Engebrethsen 2010). Selbusjøen is known to thermally stratify (Tvede 2001), which occurs well below the Bratsberg intake at a depth of approximately 15 meters. This indicates that the thermo-peaking within this system will not be as severe as if the intake were located lower within the reservoir (Sherman 2007). It should be noted that internal waves (seiches) have been registered in Selbusjøen (Tvede 2001), potentially creating spikes in the temperature measurements.

2.2 Model tools and input data

In order to investigate the changes in water temperatures introduced by changes in operational regime, the model system HEC-RAS (Brunner 2010) was applied. For unsteady flow, HEC-RAS solves the Saint-Venant Equation in one-dimension using an implicit, finite difference method. The hydrodynamic model is calibrated through a systematic tuning of bed roughness coefficients (Manning's n). The water temperature is simulated with an advection-dispersion module, using the Quickest-Ultimate explicit numerical scheme (Jensen 2004) to solve the one-dimensional advection-dispersion equation on mass and energy. It should be noted that heat fluxes are limited to atmospheric exchange, assuming no conduction from the bed, and no convection from groundwater interaction.

The succeeding impacts on salmon egg development was evaluated by a simplistic temperature-driven model (Crisp 1981; Crisp 1988). The CRISP model relates salmonid life-stage development from egg to alevin to parr to degree-day accumulation. The degree-day accumulation is calculated as a time integral of positive water temperatures. The changes in ice formation were evaluated by a set of criteria (Daly 1991; King 2012) for ice formation, i.e. super cooled water (0 ^{o}C) should be present, air temperatures should be less than -6 ^{o}C, and the negative heat flux should be greater than -100 Watts/m^{2}.

The main input data to the study is bathymetric data on the river, discharge and water temperature data for calibration, and meteorological data for the energy balance module of HEC-RAS (Table 2.1). Data is compiled from public sources, the hydropower utility operating Bratsberg and Leirfossen hydropower plants (Statkraft) and own measurements (NTNU).

Table 2.1. Input data used in the assessment of water temperature changes in Nidelva introduced by alternative hydro-peaking regimes.

Analytical tool	Data type	Data source	Time resolution
HEC-RAS Hydro-dynamic module	Water flow/levels	Norwegian Water and Energy Directorate (NVE) and Statkraft.	1 hour
HEC-RAS Hydro-dynamic module	Cross-sections (bathymetry)	Various measurement campaigns at NTNU.	Not relevant
HEC-RAS Energy Balance module	Meteorological data	Met.no (Voll meteorological station)	6 hours
HEC-RAS Energy Balance module	Water temperature (in river)	Own measurements	15 mins
HEC-RAS Energy Balance module	Water temperature data at upstream boundary	Calculated	Flexible
CRISP	Water temperature	HEC-RAS output	Flexible
ICE production	Water temperature	HEC-RAS output	Flexible

As measurements of water temperatures from Selbusjøen for the period of our study was not available, input describing the boundary conditions, i.e. input water temperature at upper end, had to be generated. It was assumed that temperatures at the upstream boundary of the model can be described by a discharge weighted average of the temperature of water in the bypass reach and in the Bratsberg discharge. The temperature records for flow through Bratsberg and flow along the bypass reach were produced through a deconvolution of the bulk temperature signal at the Rathe gauge using 507 hydro-peaking events over the calibration period (see details in King 2012).

2.3 Calibration of hydro-dynamic and energy balance module

River bed roughnesses (Manning n) were used to manually calibrate the hydraulic component of the HEC-RAS model for three observed steady state water surface profiles. The calibrated roughness ranged from 0.006 to 0.12 and produced water surface profiles that fit the observations well (Figure 2.3). Figure 2.3 (map to the right) provides a schematic of roughness values and explanations for the elevated values. As all three water surface profiles were used for calibration, the hydraulic module did not undergo validation. The statistical results of the goodness-of-fit calculation also confirm a good calibration performance (Table 2.2).

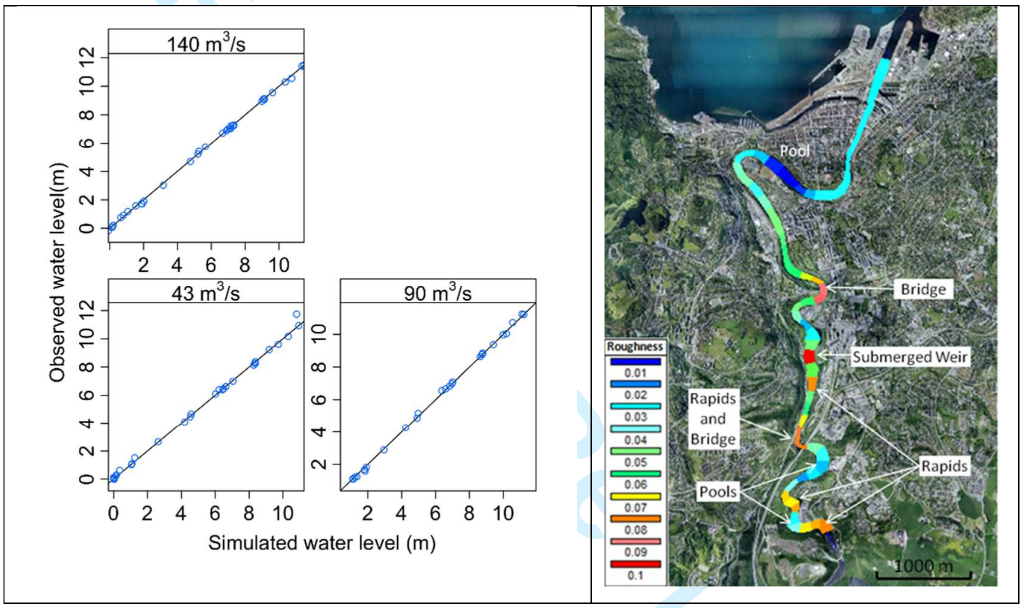

Figure 2.3. Observed and modeled water surface elevation in meters over sea-level [m.a.s.l.] for discharges of 140 m^3/s (upper left), 90 m^3/s (lower right) and 43 m^3/s (lower left). The straight lines across the panels represent perfect fit between the observations and simulation results. The map to the very right presents calibrated Manning's numbers for each sections. Red color indicates high roughness values and blue color indicates low roughness values.

Table 2.2. Goodness-of-fit of between observed and simulated water levels, expressed by Nash-Sutcliffe (R2) and Pearson's correlation coefficient. The calibration results are presented graphically in Figure 2.3.

	Water flow [m^3/s]		
Statistical criteria	43	90	140
Nash-Sutcliffe (R2)	0.997	0.999	0.999
Pearson's correlation coefficient	0.999	0.999	0.999

The energy balance model was calibrated through manual adjustment of three free parameters pertaining to atmospheric attenuation, thermal diffusivity, and wind speed at the water surface (King, 2012). The calibration was carried out by calculating water temperature time-series and cumulative degree-day accumulation profiles at the midstream and downstream locations for the period October 7, 2010 - May 27, 2011 (Figure 2.4). The period September 1, 2012 – November 4, 2012 was used for validation purpose.

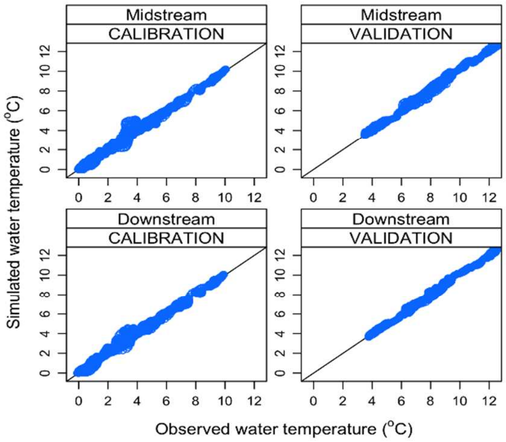

Figure 2.4. Results of the calibration process of the water temperatures in the panels to the left and validation in the panels to the right. The straight lines across the panels represent perfect fit between the observations and simulation results.

The energy model produced average deviations less than 0.1°C for both the calibration and validation periods (Table 2.3). The 'typical error', expressed as the mean residuals, are less than 0.01 ^{o}C at midstream and downstream locations during both the calibration and validation periods. The largest deviation between the model results and observations is slightly more than 1 ^{o}C and is an over-estimation at the downstream location during the calibration period. This must be considered very good, which is also confirmed by the accompanying statistics. (Table 2.4).

Table 2.3. Calibration and validation residuals from the energy balance model at the midstream and downstream locations. The number of data points for the calibration was n=334561, while n=20161 for the validation.

	Calibration Residuals [^{o}C] Oct. 7 2011- May 27 2012				Validation Residuals [^{o}C] Sept. 1 2012 – Nov. 4 2012			
Location	Min.	Mean	Max.	St. Dev.	Min.	Mean	Max.	St. Dev.
Downstream	-1.01	-0.039	1.69	0.12	-0.66	0.05	0.69	0.14
Midstream	-0.85	-0.089	1.26	0.10	-0.49	-0.026	0.51	0.11

Table 2.4. Goodness-of-fit of between observed and simulated water temperatures, expressed by Nash-Sutcliffe (R2) and Pearson's correlation coefficient. The calibration results are presented graphically in Figure 2.4.

	Midstream location		Downstream location	
Statistical criteria	Calibration	Validation	Calibration	Validation
Nash-Sutcliffe (R2)	0.996	0.995	0.997	0.999
Pearson's correlation coefficient	0.998	0.998	0.999	0.999

2.4 Identification of hydro-peaking and thermo-peaking events

In order to quantify the hydro-peaking and corresponding thermo-peaking events, anthropogenic hydro-peaking activity had to be separated from natural discharge fluctuations. The rate of change in discharge was calculated as the difference between consecutive discharge values for the Bratsberg and instream discharge records and sorted according to the occurrences of magnitudes of rates of change (cubic meters per second per hour). Based on graphical plots, hydro-peaking was assumed to occur for deviations of 20 m^3/s/hr or greater, which was confirmed by manual control of discharge data (see details in King 2012). This subset of data was later used for comparing the severity of hydro-peaking with the severity of thermo-peaking.

3 Definition of future scenarios

In order to establish a set of scenarios for future operation of the hydropower plants in Nidelva, a study on a possible massive installation of wind power in the North Sea was examined (NOWITECH 2013) and adapted for our purpose. In NOWITECH (2013), the off-shore installation of approximately 100,000 MW wind power production capacity was coupled with observed and modelled wind data for the period 2000-2006. From these wind power simulations, a trend showing lower production in the period April to September/October was found (NOWITECH 2013). Hydro-power production scenarios were defined to offset the projected reduction in electricity production from windpower. The currently installed capacity in the hydropower plants and the minimum flow requirements in Nidelva were considered unchanged, i.e. 150 m^3/s and 30 m^3/s, respectively.

Scenario A – FullSpring: In this scenario, production through Bratsberg is held at zero during periods of high wind production (October through March) and raised to full production capacity in April (Spring) when a drop in wind power production occurs. Full production is maintained as long as possible until there is only enough water in the reservoir to meet minimum flow requirements (30 m^3/s) for the rest of the year. At this point Bratsberg production is dropped to zero, allowing minimum flow requirements for the entire river from the reservoir to the fjord to be met through discharge along the river pathway. The discharge arriving through the river pathway is kept the same as had been observed for the base-line period (October 2010 throughout October 2011) and is not allowed to fall below 30 m^3/s.

Scenario B – FullSummer: This scenario is identical to FullSpring, with the exception that full production does not start until the beginning of June. This strategy conserves production water until the period where the wind power production is historically at its lowest level, and has hence a different operational risk profile.

Scenario C – Dynamic2006: This scenario utilized a single year (2006) of wind power production observations from the North Sea to capture the weekly scale of production fluctuation, and has hence a larger variability than the data averaged over a 7 year period. The production in Bratsberg was modelled to off-set the periods with low wind power production, typically a few days of hydropower production at a time.

For the scenarios the total/maximum amount of water in reservoir Selbusjøen available for discharge was 2.43 billion m^3. This was estimated as the sum of the minimum required flow for the reach between Leirfoss and the reservoir and the annual discharge through Bratsberg observed in the base-line period. This volume was used to determine the termination of the scenarios A and B, and was set as a maximum value that could not be exceeded in scenario C. The discharge at the Rathe gauge was held between 30 and 300 m^3/s for all scenarios.

4 Results

4.1 Analysis of the current situation (observed data)

The record of river temperature ranged between 0 and 16 ^oC over the study period (Figure 4.1), where the highest temperatures are recoded in late July and August. The temperatures were close to 0 ^oC during most of the winter, and is below 5 ^oC until June.

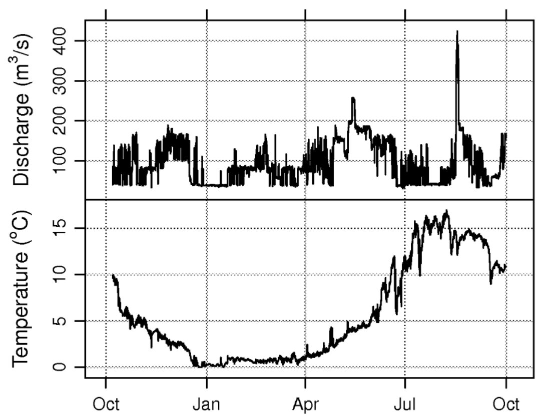

Figure 4.1. Recorded discharge and water temperatures at Rathe gauge during the period October 2010 through October 2011.

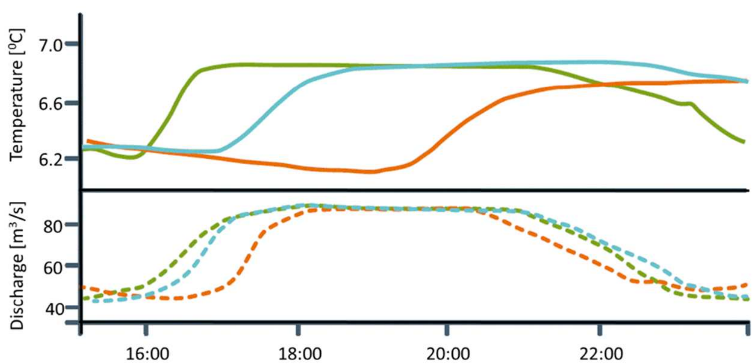

Figure 4.2. Discharges and corresponding water temperatures at three different locations, i.e. Rathe in the upstream end (green) and the midstream (light blue) and downstream (orange) locations during October 14, 2012. A time-lag in the water temperature data compared to the water flow data can be observed.

A time lag in the thermo-peaking wave compared to the hydro-peaking wave can be observed in the measured data (Figure 4.2), and the lag increases with the distance from where the hydro-peak is released into the river, which is in line with the theoretical findings of Toffolon et al. (2010). As there are now tributaries along the modelled part of the river of sufficient volumes that could possible delay the speed of the thermo-peaking wave (as described by Brown & Hannah, 2008). A physical understanding of this phenomenon as observed in Nidelva is that the celerity of the wave has a higher velocity than the water. The water with a different temperature will reach the gauging stations slightly later than the increase in water level, which is seen as a time lag between the water level change and the temperature change.

A seasonal context for the thermo-peaking is displayed by the distribution of thermo-peaking responses (Figure 4.3). The thermo-peaks were identified, as event based alterations in river temperature associated with hydro-peaking events (as described in Section 2.4). The identified hydro-peaking events are divided into 231 wintertime, 92 summertime, and 183 combined spring and fall events. Spring and fall events have the smallest magnitudes. The winter and summer events have larger magnitudes, and opposite signs in thermo-peaking. The analysis shows that thermo-peaks and hydro-peaks are positively related in the winter period, and negatively related in the summer period, and the thermo-peaking responses are increasing in severity when the magnitude of the hydro-peaking increases. The severity in hydro- and thermo-peaking are expressed as deviations from average discharges and average water temperatures (over the peaking events), respectively (Figure 4.3).

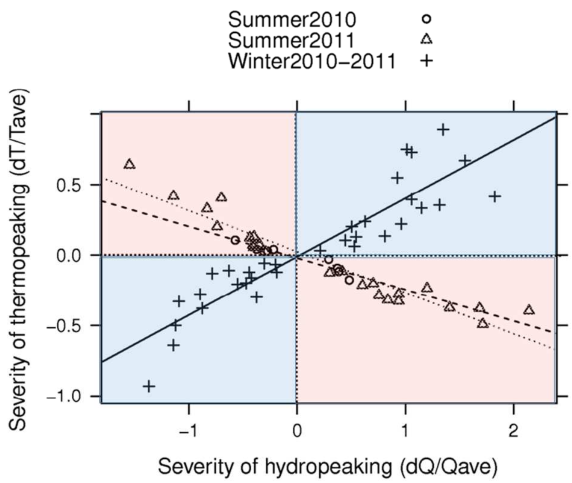

Figure 4.3. The degree of thermo-peaking in response to hydro-peaking during summer and winter period. The two panels on the left side describe changes during down-ramping (reductions in flow) while the two panels to the right describe up-ramping (increased flows). The upper parts describe increase in water temperature, while the lower part decrease in water temperature with changes in flow. The red parts represent the summer situation, while the blue parts the winter situation.

4.2 Simulation results from future production scenarios

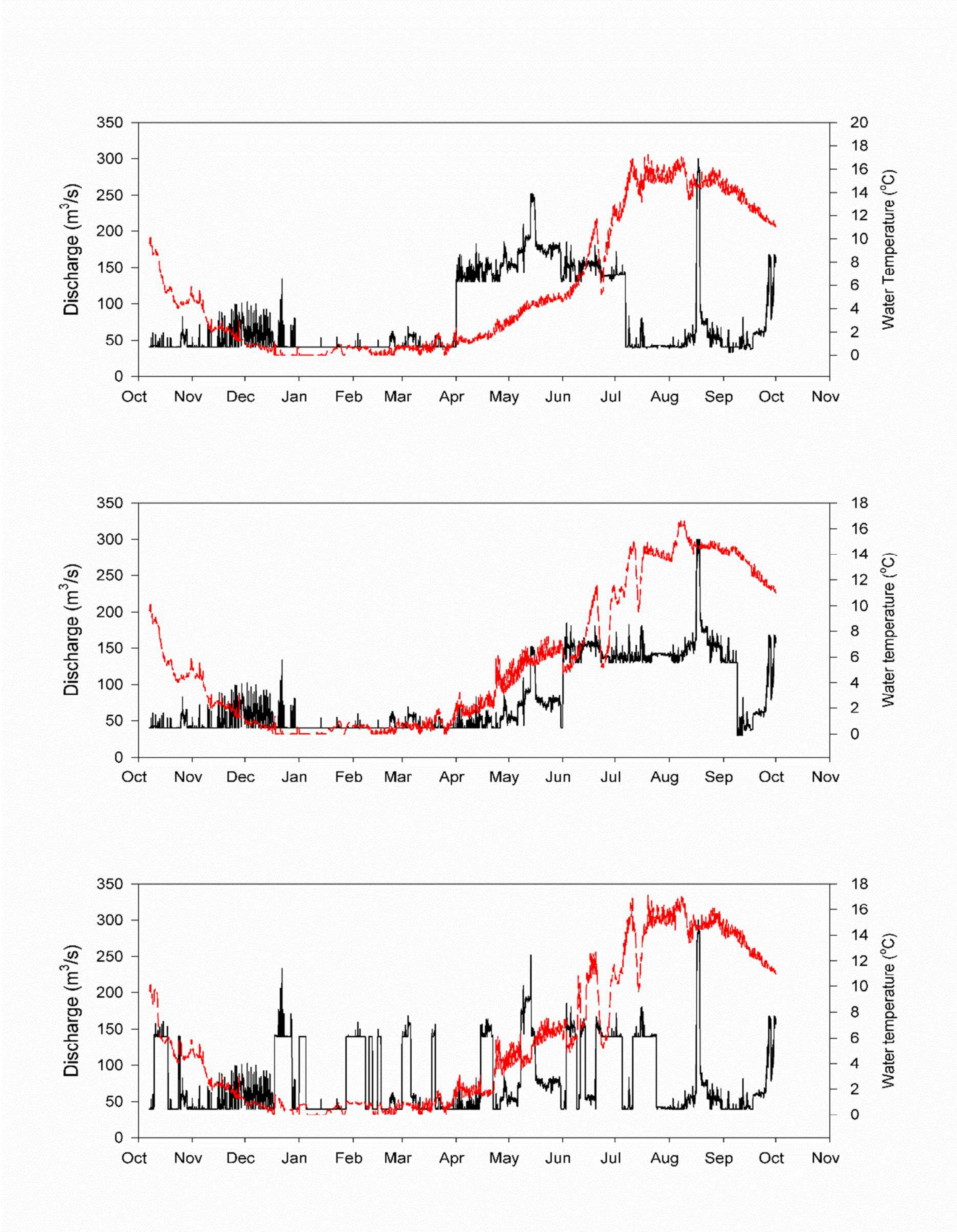

Figure 4.4. Modeled discharges (blue lines) and water temperatures (red lines) at the downstream location during the scenarios FullSpring (at the top), FullSummer (in the center) and C Dynamic2006 (in the lowest graph). The future scenarios are simulated based on input data from the period October 2010 – October 2011.

The resulting discharges and water temperatures for the three defined scenarios are calculated (Figure 4.4). In both scenarios FullSpring and FullSummer (two upper panels), production during the winter is very restricted due to the scenario definitions, while in scenario Dynamic 2006 power is produced in bulks in the period January – April.

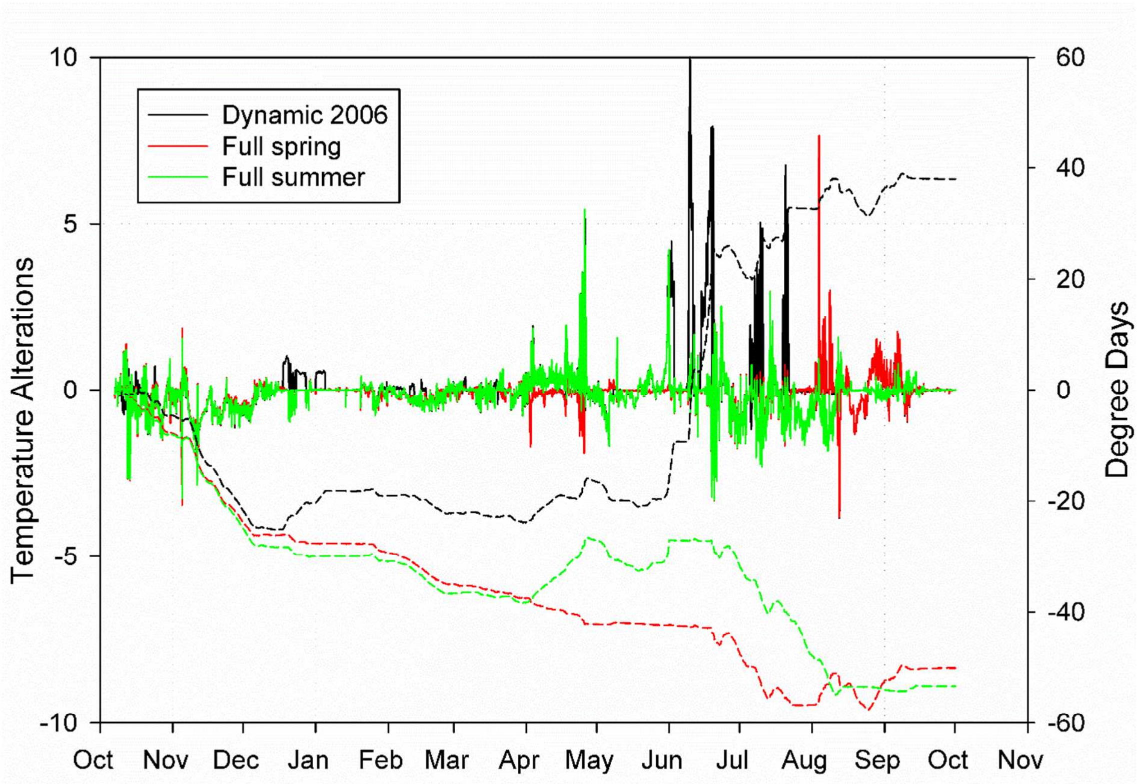

Figure 4.5. Deviations between observed (base-line) and simulated temperatures at the downstream location for the scenarios FullSpring (green solid line), FullSummer (red solid line) and Dynamic2006 (blue solid line). The future scenarios are simulated based on input data from the period October 2010 – October 2011. Accumulative deviations (in degree-days) are plotted against the secondary y-axes (dashed lines).

Day-to-day deviations between base-line and the three scenarios are calculated as accumulated deviations in degree-days (Figure 4.5). On specific dates during the summer the difference in water temperatures can be very large, i.e. up to 10 ^{o}C between the base-line and Dynamic2006-scenario. The is because only minimum flow is released these specific days and heating from warm weather occur in Dynamic2006, while larger volumes of water are present in the river during the base-line, slowing down the heating effect on the temperatures.

By studying the graphs with the accumulated degree-days it is interesting to see that all three scenarios ‘lose’ degree-days in the beginning of the study period, and FullSpring and FullSummer basically follow the same pattern the whole period and end up ‘producing’ approx. 50 degree-days less than the base-line. The Scenario Dynamic2006 catches up the lost degree-days during the early summer and ends up approx. 40 degree-days higher than the base-line.

4.3 Impacts on salmon egg development and ice production

The CRISP model (Crisp 1981; Crisp 1988) is essentially a transformed version of degree-day accumulation, using water temperature as its only driving parameter. This model was fed with output from the energy balance model to calculate hatching dates associated with each discharge scenario. In each case the spawning date was set to November 5th. The changes in the development are illustrated by alterations in hatching and swim-up dates (Table 4.1).

Table 4.1. Crisp model results: impact of discharge scenarios on salmon egg development.

Scenario	Hatch Date	Alteration in hatch date	Swim-up date	Alteration in swim-up date
Base-line	10 May	-	30 June	-
FullSpring	14 May	+ 4 Days	2 July	+ 2 Days
FullSummer	14 May	+ 4 Days	2 July	+ 2 Days
Dynamic2006	12 May	+ 2 Days	25 June	- 5 Days

As the hatching happens during the spring and before Dynamic2006 catches up the 'lost degree-days', this life-stage is slightly delayed (2-4 days) for all scenarios (Table 4.1). When it comes to swim-up dates, the scenarios FullSpring and FullSummer are still behind the base-line, while the swim-up will happen a few days earlier in the Dynamic2006 scenario. The change must, however, be considered very small, and probably well within the uncertainty of the model predictions.

It is also worthwhile noting that even though the scenarios FullSpring and FullSummer loses approximately 40 degree-days to the time of hatching (Figure 4.5), this represents only losing 4 days to hatching (Table 4.1). This is explained by the formulations of egg development in the CRISP model (Crips 1981; Crisp 1988), which basically transforms water temperatures into progressions (in percent) towards hatching date, and further into swim-up date.

Table 4.2. Ice formation potential for observed and simulated discharge scenarios.

	Base-line	A-FullSpring and B-FullSummer	Dynamic2006
No of events with ice potential	9	19	10
Latest event	4 January	24 February	24 February
Min. ice event [hours]	1.75	1	1.5
Max. ice event [hours]	86	103	19
Mean ice event [hours]	15	13	6
Median ice event [hours]	5	5	5
Sum [Days]	5.8	10.3	2.6
Change [Days]	-	+4.5	-3.2

The results indicate that the scenarios FullSpring and FullSummer will lead to increased number of events with ice formation (Table 4.2). This is explained by the scenario definitions, where water is prioritised for hydropower production during spring and summer, respectively. This will reduce the volumes of water in Nidelva during the winter, thus requiring less heat loss before the water reaches 0 ^{o}C. The same is not seen in the Dynamic2006 scenario, as this scenario allows for periods of elevated discharge through the winter. The intermittent nature of discharge in the Dynamic2006 scenario leads to more, shorter, potential freezing events, and has an overall effect of decreasing the freezing potential for the examined year.

5 Discussion

The severity of the thermo-peaking closely follows the severity of the hydro-peaking. The magnitudes of the thermo-peaks are limited, with the majority of the water temperature changes within the range of +/- 2.0 ^{o}C in one cycle of peaking operations. Comparing these values to prior studies on thermo-peaking (e.g. Zolezzi et al. 2011) the temperature variations in Nidelva are small, while other studies have found large thermal heterogeneity across the basin (spatial dimension). In our data, there is a distinct trend in the thermo-peaking, that warming of Nidelva happens with increased discharges in the winter and cooling with increased discharges in the summer, with a transition period between with less severe thermo-peaking. The transition between seasonal regimes occurred in our data in March and September, while the maximum thermo-peaking responses were observed in November and June. Zolezzi et al. (2011) found that warm thermo-peaking occurred from September to January, and cold thermo-peaking from March to July. Their results were compared with an unregulated situation, while our observations of thermo-peaking are analyzed and related to the severity of the hydro-peaking waves.

The model tools applied proved their capabilities to simulating hydro-peaking operations and the effect on water temperatures. A longer period of data from more locations in the model domain would have further increased the confident in the model setup, i.e. increased the certainty that the calibrated parameters would be representative for a larger set of combinations of flow and climatic conditions. The temporal resolution of observed discharge data could have been better as we have 60 minute resolution in water level/flow data, while there is a 15 minutes temporal resolution in the water temperature data. The time step of the data clearly affects the precision in the description of the hydro-peaking (Sauterleute & Charmasson 2014; Carolli et al. 2015) as longer time steps tend to smoothen out the effects of rapid changes in parameters describing the hydro-peaking cycle. Along the 8 km river stretch we have water temperature data from 3 locations for the calibration period and 6 locations for the validation period, and discharge data for the upstream boundary. Studies of hydro-peaking introduce challenging needs for data with fine resolution (especially temporal resolution), but the overall data situation in Nidelva is very good compared to the majority of regulated rivers in Norway. We believe that in most cases where hydro-peaking and effects on water temperature are to be studied, new measurement campaigns must be carried out.

The three simulated scenarios are defined in a fairly simplistic way, in particular the FullSpring and FullSummer scenarios. As the scenarios are evolved from large scale-scenarios of a massive off-shore installations of wind power, possible decades ahead in time, it is impossible to read out of these studies how this might affect the individual hydropower plants in Norway. Only indications of changes in hydropower operation can be assessed, with several critical assumptions defined. Within this context the three scenarios for the hydropower operation in Nidelva was made. Despite their simplistic formulation, they represent a diverse set of hydropower operation strategies. The market driver/overall operational strategy behind the scenario FullSpring is that it is better to produce electricity as soon as the market price increases in the spring to avoid a potential situation ('risk') where the water is stored/saved in the reservoir for later production and that the expected further reduction in wind power production does not happen, i.e. the wind persist in the North Sea throughout the Summer and the saved water cannot be realised for production in a period with high electricity price. The overall operational strategy behind FullSummer is that it is more profitable to save the production water until the period where the wind power production is historically at the lowest level. It is potentially 'more money to earn' by saving the water to a period when it is less wind/lower wind power production and highest price, even though there is a risk that the wind will persists also throughout the summer, i.e. there is a higher risk profile in FullSummer than the FullSpring scenario. The scenario Dynamic2006 represents a situation where the variability is much higher as it follows the drops in the wind power production during a year with typical climatic (wind) conditions, giving a more dynamic production pattern. We believe that these three scenarios will cover a range of possible operational strategies and that the results illustrate the range of output with respect to water temperatures large scale development of wind power might give.

The scenario results show that two of the scenarios (FullSpring and FullSummer) produce approx. 50 degree-days less than the base-line where 35-40 of the 50 degree-days are in the period November throughout February while the last 10-15 degree-days are 'lost' during the summer. The third scenario (Dynamic2006) achieves 40 degree-days more than the base-line. This scenario actually 'loses' 20 degree-days during the period November to May, but compensate this loss and produce 40 degree-days more from early June until the end of September, a very important period for salmon growth.

The degree-days (accumulated water temperatures) are transformed into impacts on salmon egg development and illustrate how impacts can be presented in a way that is closer to those questions management authorities responsible for environmental impacts in regulated rivers ask than the results on water temperatures alone. As such, these results are interesting and indicate that the impacts on salmon development schedules might vary only slightly under very different flow regimes. This raises the interesting point that under the FullSpring and FullSummer scenarios alevin will swim up into higher flows than those observed under the baseline scenario. Whether or not these impacts should be considered negative or positive to the ecosystem will depend on the environmental management goals of the river (e.g. to strengthen the salmon population), and the impacts on other ecosystem elements, like for instance the presence and composition of invertebrates. In the study by Onstad (2011) reactions to hydro-peaking amongst salmon fishers (recreational use) in the river Nidelva River were analysed, and it appears that the main concern regarding water temperatures is the low (average) temperatures and not the temperature fluctuations. These salmon fishers also report that they have experienced larger rapid changes in water temperatures than we found in our observations (Onstad 2011), which also might be explained by seiches (internal waves) in Selbusjøen (Tvede 2001).

Changes in water temperatures are also transformed into changes in ice formation, by use of fairly simple physical criteria. These criteria are based on modelled water temperatures and heat exchange and the observed air temperatures, and do not consider ice-break-up events triggered by for instance changes in water flows. A more sophisticated analysis than our criteria-based approach should be applied to Nidelva in a real management situation, but water temperature simulations would still form the basis for further assessment of ice formation.

Thermo-peaking might change the natural thermal regime in a river in time-scales ranging from very short (minutes), to sub-daily (hours), days, seasons or even decades (e.g.Webb and

Nobilis 2007). Our water temperature data has a 15 mins time resolution and can support the analysis from the very fine to seasonal time-scale. Most of the published studies on thermo-peaking compare changes in water temperatures with an unregulated situation (Vanzo et al. 2015), studying the phenomena (Steel & Lange, 2007), or explaining anomalies in long-term water temperatures trends with river regulations (Webb & Nobilis 2007). In our study, we have compared the present operational regime (base-line), which must be characterized as being hydro-peaked, with three scenarios for possible changes in the hydro-peaking regulations, which make direct comparison with other studies difficult.

Models are simplified representations of the world and will introduce inaccuracies and uncertainties when applied on real world problems. The introduction of uncertainties is related to both the input data to the model and the process representations. Most of the input data to the models are, however, assumed being of high quality, i.e. the meteorological data and the river bathymetry, as well as the discharge, water level and water temperature data used for calibration. This is also, to some extent, confirmed by the good calibration results. The input data determining the upstream boundary conditions is probably more uncertain as they are calculated by a discharge-weighted approached based on historical data. Better data on water temperatures from the inlet of the hydropower tunnel in Selbusjøen would have been a preferred situation. It is also assumed that the proposed scenarios will not introduce any changes in circulation or stratification in Selbusjøen compared to the base-line situation. This is a critical assumption as the water temperature downstream of Selbusjøen is to a large extent determined by this upstream boundary condition (Brown & Hannah 2008). Ideally, a lake/reservoir simulation model should have been configured to provide input data to HEC-RAS.

HEC-RAS assumes no interaction of water or heat between the river and the groundwater. Casas-Mulet et al. (2015) carried out measurements of water temperatures and flow in the nearby river Lundesokna exposed to hydro-peaking and found very small differences in water temperatures in the river and the hyporheic zone (groundwater). As such, simplifications on the heat exchange with the bottom, lateral inflow from groundwater and small tributaries do not seem to affect the calibration results, which are considered representing only minor sources of errors in the simulated scenarios. There are no large tributaries to Nidelva along the model section. The largest single source entering Nidela is Leirelva, with an average discharge of 0.7 m^3/s (NVE Atlas 2016), which is less than 1% of the average flow in Nidelva.

The CRISP model is not validated against real data on egg development in Nidelva, but simply based on transfer of fitting parameters from the neighbour river Orkla. Comparing calculated values/dates on egg development with real data in Nidelva would definitely increase the confident in the model results of our study.

6 Conclusions

Based on observations of hydro- and thermo-peaking events in Nidelva River in mid-Norway, we conclude that:

- hydro-peaking operations introduce thermo-peaking, both winter and summer even if they are fairly small.
- during the summer an increase in flow causes a decrease in water temperature and vice versa. During the winter period, an opposite response can be observed as an increase

in flow causes an increase in water temperature and a decrease on flow will lead to a decrease in water temperature.

Our simulations of three alternative future scenarios leading to possible new hydro-peaking regimes show that:

- fairly small changes are expected in water temperatures compared to present day's operational regime, measured in accumulated degree-days. The model simulations predict a reduction in the range of 50 degree-days for two of the scenarios and an increase in approximately 40 degree-days for the third scenario (Dynamic2006).
- transforming the changes in water temperatures into changes in salmon egg development, the hatching date will be 2-4 days delayed for all three scenarios. The swim-up date will be approx. 2 days delayed for the scenarios FullSpring and FullSummer, and 5 days earlier for the scenario Dynamic2006.

We believe that tools such as HEC-RAS with its modest data requirements, coupled with biological assessment methods such as the CRISP model and ice formation criteria, will provide useful and relevant information when impacts of different operational regimes of hydropower plants are examined. In the light of upcoming revisions of hydropower concessions (in Norway), implementation of the EU Water Framework Directive (Europe) and development of new hydropower/pumped storage plants (world-wide), tools capable of supporting decision-making are of major importance.

Acknowledgement

This paper is based on the results from a master's thesis by Tyler King, submitted to the University of New Hampshire in partial fulfilment of the requirements for the Degree of Master of Science in Hydrology, under the supervision of J. Matthew Davis and Anne Lightbody. The majority of the work was carried out during an exchange with the University of Science and Technology (NTNU) in Trondheim, Norway and supervised by Knut Alfredsen. The work was scientifically co-ordinated with the research carried out in the EnviPEAK-project, funded by the Research Council of Norway. EnviPEAK is organized under the research centre CEDREN (Centre for Environmental Design of Renewable Energy – www.cedren.no, contract 201779). We would like to thank two anonymous reviewers for providing very useful feedback on earlier versions of the article.

7 References

Bakken TH, Zinke P, Melcher A, Sundt H, Vehanen T, Jorde, K, Acreman M. 2012. Setting environmental flows in regulated rivers. SINTEF Report Serial No. TR A7246. ISBN 978-82-594-3529-3.

Berland G, Nickelsen T, Heggenes J, Økland F, Thorstad EB, Halleraker J. 2004. Movements of wild Atlantic salmon parr in relation to peaking flows below a hydropower station. River Research and Applications 20: 957–966.

Bradford M J. 1997. An experimental study of stranding of juvenile salmonids on gravel bars and in side channels during rapid flow decreases. Regulated Rivers: Research and Management 13: 395–401.

Brown LE, Hannah DM. 2008. Spatial heterogeneity of water temperature across an alpine river basin. Hydrological Processes 22: 954–967. DOI: 10.1002/hyp.6982.

Brunner GW. 2010. HEC-RAS River Analysis System User's Manual Version 4.1. US Army Corps of Engineers Institute for Water Resources Hydrologic Engineering Center, Davis, CA.

Bruno MC, Siviglia A, Carolli M, Maiolini B. 2013. Multiple drift responses of benthic invertebrates to interacting hydropeaking and thermopeaking waves. Ecohydrology 6: 511–522, DOI: 10.1002/eco.1275.

Caissie D. 2006. The thermal regime of rivers: a review. Freshwater Biology 51 (8): 1389-1406.

Carolli M, Vanzo D, Siviglia A, Zolezzi, G, Bruno MC, Alfredsen K. 2015. A simple procedure for the assessment of hydropeaking flow alterations applied to several European streams. Aquatic Sciences 77:639–653. DOI 10.1007/s00027-015-0408-5.

Casas-Mulet R, Alfredsen K, Hamududu B, Timalsina NP. 2015. The effects of hydropeaking on hyporheic interactions based on field experiments. Hydrological Process 29: 1370–1384. DOI: 10.1002/hyp.10264.

Crisp DT. 1981. A desk study of the relationship between temperature and hatching time for the eggs of five species of salmonid fishes. Freshwater Biology 11 (4): 361-368.

Crisp DT. 1988. Prediction, from temperature, of eyeing, hatching and swim-up times for salmonid embryos. Freshwater Biology 19 (1): 41-48.

Coutant CC. 1999. Perspective on temperature in the Pacific Northwest's fresh water. Tech. rep., Environmental Sciences Division, Oak Ridge National Laboratory.

Daly SF. 1991. Frazil ice blockage of intake trash racks. Tech. rep., Cold Regions Research and Engineering Laboratory.

Engebrethsen T. 2010. Melding om oppstart av planleggingsarbeidet for nye Svean kraftverk. Tech. rep., Statkraft.

Fremstad E, Thingstad P. 2007. Nidelva, Trondheims hjerte. Tech. rep., NTNU. Vitenskapsmuseet: Seksjon for naturhistorie.

Gabrielsen RH, Grue J. 2012. Norwegian Energy Policy in Context of the Global Energy Situation. The Norwegian Academy of Science and Letters, Oslo, Norway.

Greimel F, Zeringer B, Höller N, Grün B, Godina R, Schmutz S. 2016. A method to characterize sub-daily flow fluctuations. Hydrological Processes. DOI: 10.1002/hyp.10773. (Accepted for publication).

Hvidsten NA. 1985. Mortality of pre-smolt Atlantic salmon, Salmo salar L., and brown trout, Salmo trutta L., caused by fluctuating water levels in the regulated River Nidelva, central Norway. Journal of Fish Biology 27 (6): 711-718.

IPCC: Edenhofer O, Pichs-Madruga R, Sokona Y, Seyboth K, Matschoss P, Kadner S, Zwickel T, Eickemeier P, Hansen G, Schlömer S, von Stechow Ce. 2011. IPCC Special Report on Renewable Energy Sources and Climate Change Mitigation. Cambridge University Press, Cambridge, United Kingdom and New York, NY, USA.

Jensen MCL. 2004. Temperature modeling with HEC-RAS. Tech. rep., ASCE.

Johnsen BO, Arnekleiv JV, Asplin L, Barlaup BT, Nesje TF, Rosseland BO, Saltveit SJ. 2010. Effekter av Vassdrags-Regulering på Villaks. Kunnskapssenter for Laks og Vannmiljø.

King T. 2012. Thermal Implications of hydropeaking activity in regulated rivers. Master's thesis at the University of New Hampshire, U.S.

Maddock I, Harby A, Kemp P, Wood P. 2013. Ecohydraulics: An Integrated Approach. John Wiley & Sons, Ltd. Print ISBN: 9780470976005. Online ISBN: 9781118526576. DOI: 10.1002/9781118526576.

Moog O. 1993. Quantification of daily peak hydropower effects on aquatic fauna and management to minimize environmental impacts. Regulated Rivers: Research and Management 8: 5–14.

NOWITECH. 2013. NOWITECH Research Centre for Offshore Wind Technology. SINTEF Energy Research, Trondheim, Norway. www.sintef.no/Projectweb/Nowitech/ (Accessed 18 May, 2015).

NVE Atlas. 2016. Map-based Data provided by Norwegian Water Resources and Energy Directorate. http://atlas.nve.no/SilverlightViewer/ (Accessed 22 February, 2016).

OED (Olje og Energidepartementet). 2006. Meddelte vassdragskonsesjoner. Tillatelser meddelt i 2006. Vedlegg til St.prp. nr. 1, 20072008, Energi og vassdragsforvaltning.

Onstad O. 2011. Reactions to hydropeaking amongst salmon fishers in the river Nidelva in Trondheim-results from focus group interviews and survey. Master's thesis at Norwegian University of Life Sciences (UMB), Ås, Norway.

Randle TJ, Samad MA. 2008. Platte River in central Nebraska modeling of pulse-flow release. Tech. rep., U.S. Department of the Interior Bureau of Reclamation.

Saltveit SJ, Halleraker JH, Arnekleiv JV, Harby A. 2001. Field experiments on stranding in juvenile Atlantic salmon (Salmo salar) and brown trout (Salmo trutta) during rapid flow decreases caused by hydropeaking. Regulated Rivers: Research and Management 17: 609–622.

Sauterleute JF, Charmasson J. 2014. A computational tool for the characterisation of rapid fluctuations in flow and stage in rivers caused by hydropeaking. Environmental Modelling & Software 55: 266–278.

Schlosser IJ, Johnson JD, Knotek WL, Lapinska M. 2000. Climate variability and size-structured interactions among juvenile fish along a lake-stream gradient. Ecology 81 (4): 1046-1057.

Scruton DA, Ollerhead LMN, Clarke KD, Pennell C, Alfredsen K, Harby A, Kelley D. 2003. The behavioural response of juvenile Atlantic salmon (Salmo salar) and brook trout (Salvelinus fontalis) to experimental hydropeaking on a Newfoundland (Canada) river. River Research and Applications 19: 577–587.

Sherman B, Todd CR, Koehn JD, Ryan T. 2007. Modelling the impact and potential mitigation of cold water pollution on murray cod populations downstream of Hume Dam, Australia. River Research and Applications 23 (4): 377-389.

Steel EA, Lange IA. 2007. Using wavelet analysis to detect changes in water temperature regimes at multiple scales: effects of multi-purpose dams in the Willamette River basin. River Research and Applications 23 (4): 351-359.

Tvede AM. 2001. Nye Leirfossene kraftverk. Konsekvenser for vanntemperatur, is- og lokalklimaforhold. Statkraft Grøner Rapport 2001- N0072G-02.

Toffolon M, Siviglia A, Zolezzi G. 2010. Thermal wave dynamics in rivers affected by hydropeaking. Water Resources Research 46, W08536. doi:10.1029/2009WR008234.

Valentin S, Wasson JG, Philippe M. 1995. Effects of hydropower peaking on epilithon and invertebrate community trophic structure. Regulated Rivers: Research and Management 10: 105–119.

Vanzo D, Siviglia A, Carolli M, Zolezzi G. 2015. Characterization of sub-daily thermal regime in alpine rivers: quantification of alterations induced by hydropeaking. Hydrological Processes. DOI: 10.1002/hyp.10682.

Vehanen T, Bjerke PL, Heggenes J, Huusko A, Mäki-Petäys A. 2000. Effect of fluctuating flow and temperature on cover type selection and behavior by juvenile brown trout in artificial flumes. Journal of Fish Biology 56: 923–937.

Vinson MR. 2001. Long-term dynamics of an invertebrate assemblage downstream from a large dam. Ecological Applications 11 (3): 711-730.

Ward JV, Stanford JA. 1979. Ecological factors controlling stream zoobenthos with emphasis on thermal modification of regulated streams. In The ecology of regulated streams: Proceedings of the First International Symposium on Regulated Streams. Erie, April 18-20, 1979. Plenum Press, New York.

Webb BW, Nobilis, F. 2007. Long-term changes in river temperature and the influence of climatic and hydrological factors. Hydrological Sciences Journal 52(1): 74-85. DOI: 10.1623/hysj.52.1.74.

Zolezzi G, Siviglia A, Toffolon M, Maiolini B. 2011. Thermopeaking in alpine streams: event characterization and time scales. Ecohydrology, 4: 564–576. DOI: 10.1002/eco.132.

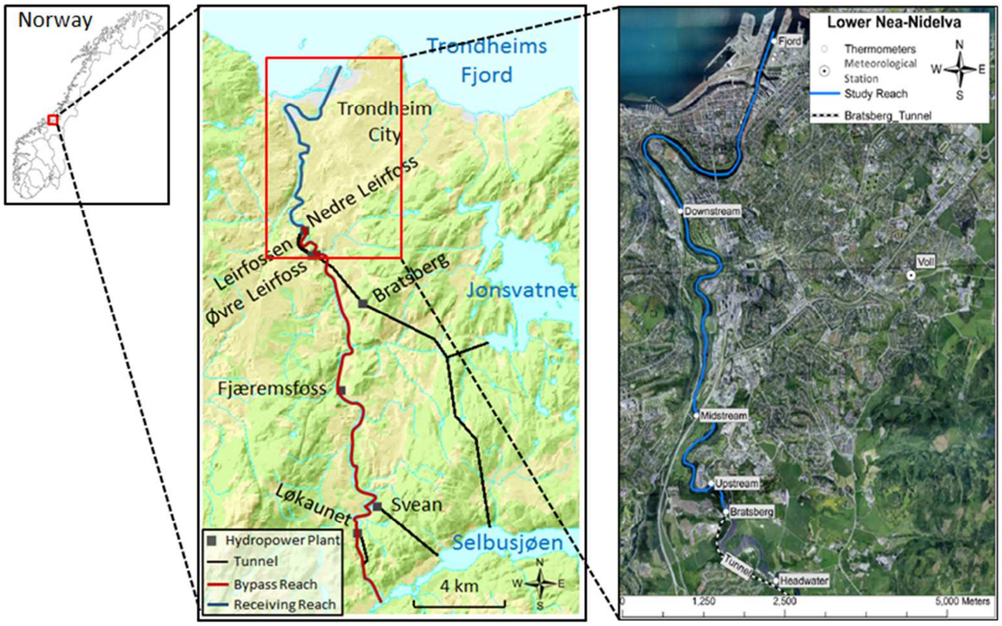

213x132mm (96 x 96 DPI)

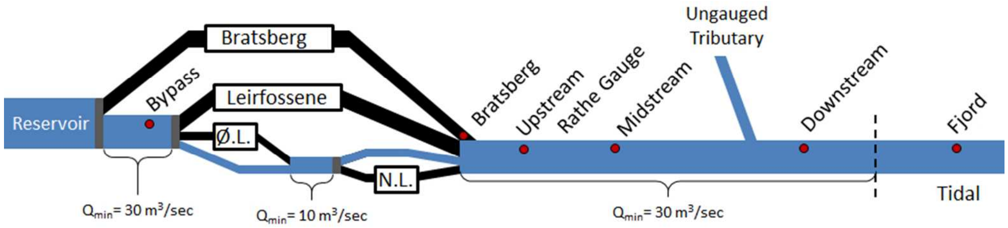

249x57mm (96 x 96 DPI)

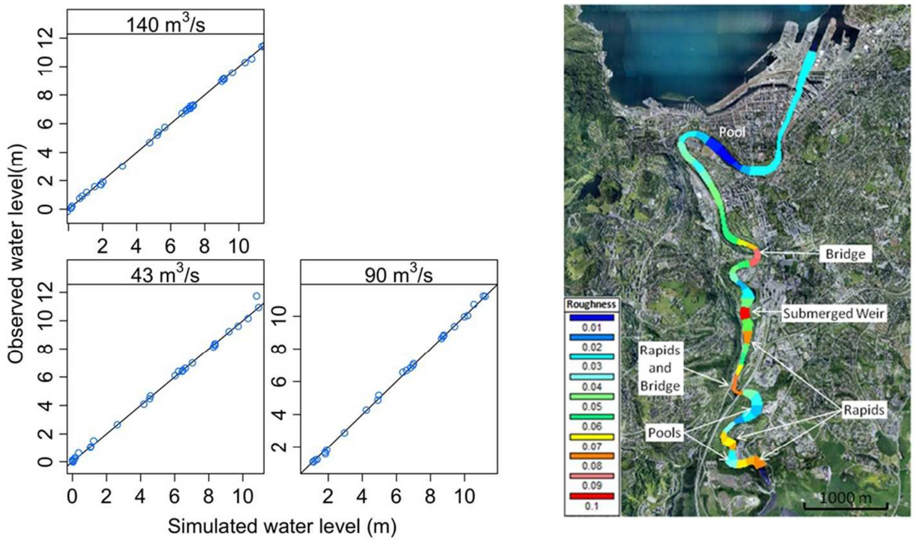

338x190mm (96 x 96 DPI)

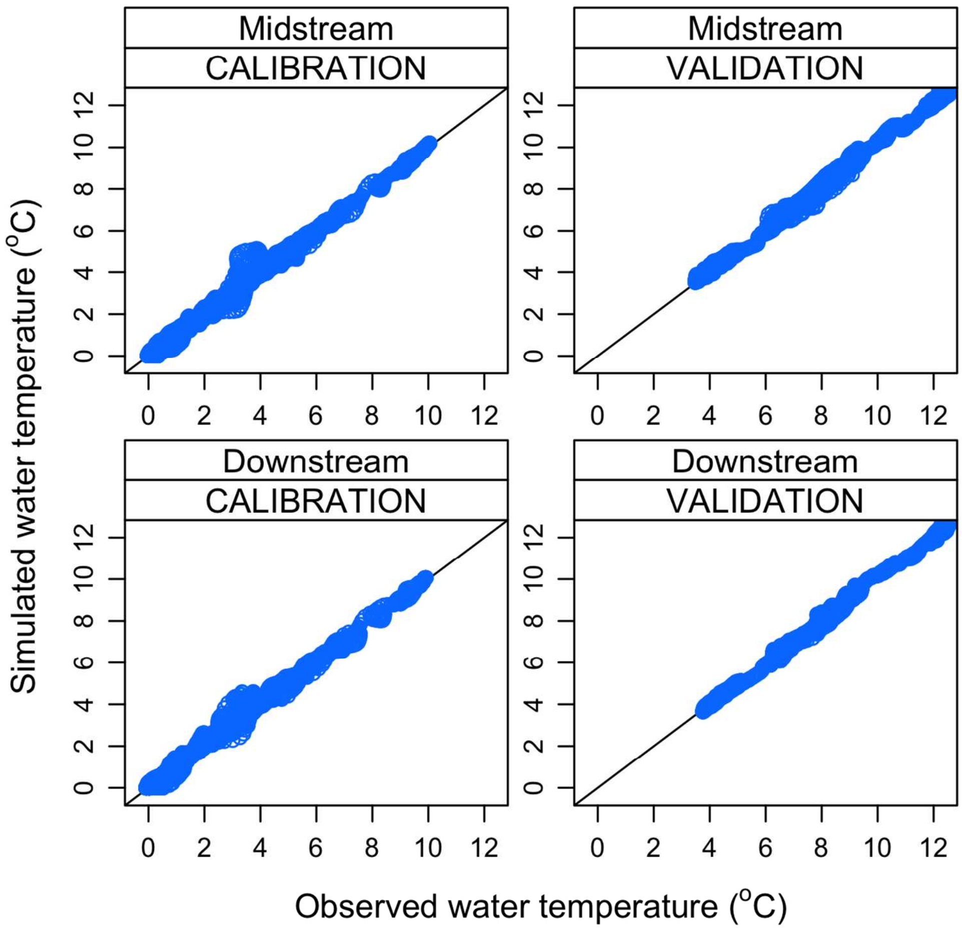

529x529mm (72 x 72 DPI)

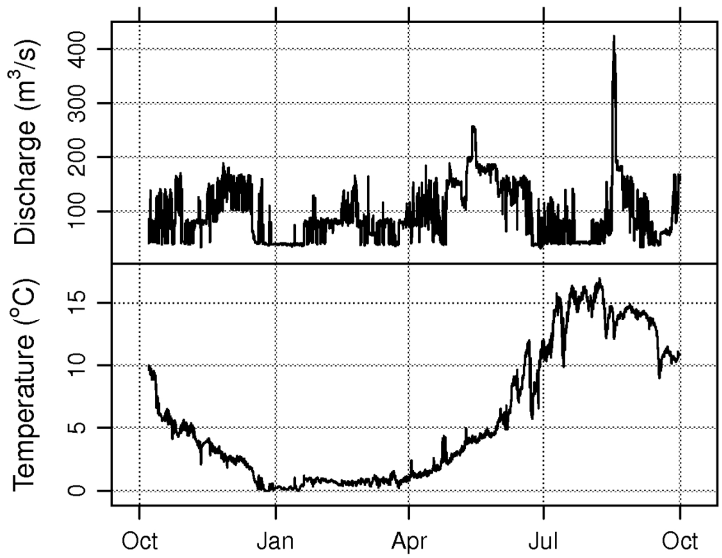

150x100mm (300 x 300 DPI)

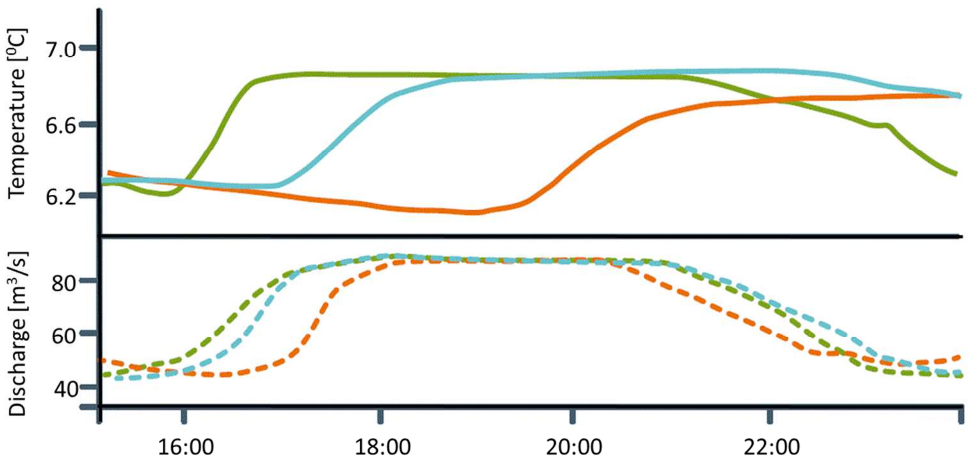

Temperature [⁰C]
7.0
6.6
6.2
Discharge [m³/s]
80
60
40
16:00
18:00
20:00
22:00

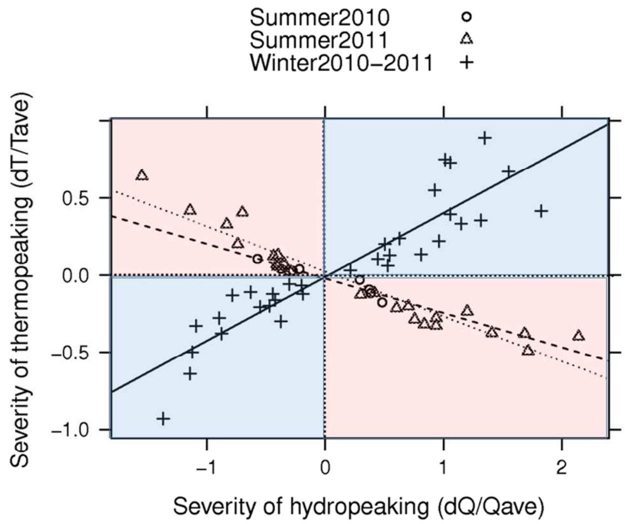
Summer2010
Summer2011
Winter2010−2011
Severity of thermopeaking (dT/Tave)
Severity of hydropeaking (dQ/Qave)
0.5
0.0
−0.5
−1.0
−1
0
1
2

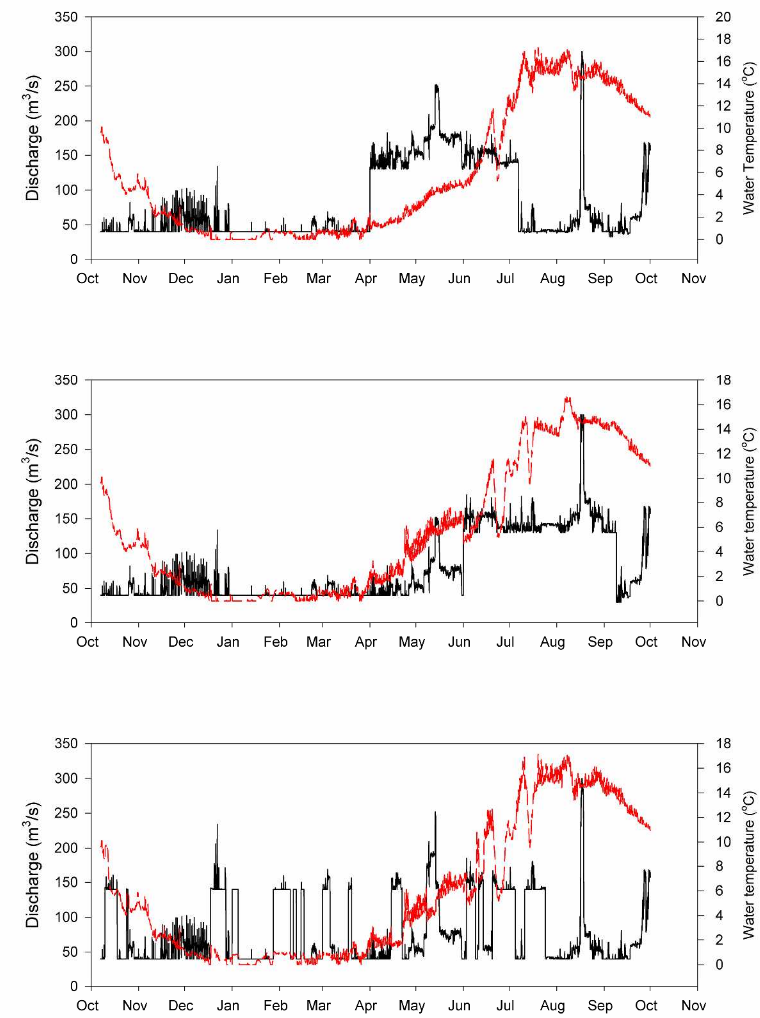

297x420mm (300 x 300 DPI)

Table 2.1. Input data used in the assessment of water temperature changes in Nidelva introduced by alternative hydro-peaking regimes.

Analytical tool	Data type	Data source	Time resolution
HEC-RAS Hydro-dynamic module	Water flow/levels	Norwegian Water and Energy Directorate (NVE) and Statkraft.	1 hour
HEC-RAS Hydro-dynamic module	Cross-sections (bathymetry)	Various measurement campaigns at NTNU.	Not relevant
HEC-RAS Energy Balance module	Meteorological data	Met.no (Voll meteorological station)	6 hours
HEC-RAS Energy Balance module	Water temperature (in river)	Own measurements	15 mins
HEC-RAS Energy Balance module	Water temperature data at upstream boundary	Calculated	Flexible
CRISP	Water temperature	HEC-RAS output	Flexible
ICE production	Water temperature	HEC-RAS output	Flexible

Table 2.2. Goodness-of-fit of between observed and simulated water levels, expressed by Nash-Sutcliffe (R2) and Pearson's correlation coefficient. The calibration results are presented graphically in Figure 2.3.

	Water flow [m^3/s]		
Statistical criteria	43	90	140
Nash-Sutcliffe (R2)	0.997	0.999	0.999
Pearson's correlation coefficient	0.999	0.999	0.999

Table 2.3. Calibration and validation residuals from the energy balance model at the midstream and downstream locations. The number of data points for the calibration was n=334561, while n=20161 for the validation.

	Calibration Residuals [^{o}C] Oct. 7 2011- May 27 2012				Validation Residuals [^{o}C] Sept. 1 2012 – Nov. 4 2012			
Location	Min.	Mean	Max.	St. Dev.	Min.	Mean	Max.	St. Dev.
Downstream	-1.01	-0.039	1.69	0.12	-0.66	0.05	0.69	0.14
Midstream	-0.85	-0.089	1.26	0.10	-0.49	-0.026	0.51	0.11

Table 2.4. Goodness-of-fit of between observed and simulated water temperatures, expressed by Nash-Sutcliffe (R2) and Pearson's correlation coefficient. The calibration results are presented graphically in Figure 2.4.

	Midstream location		Downstream location	
Statistical criteria	Calibration	Validation	Calibration	Validation
Nash-Sutcliffe (R2)	0.996	0.995	0.997	0.999
Pearson's correlation coefficient	0.998	0.998	0.999	0.999

Table 4.1. Crisp model results: impact of discharge scenarios on salmon egg development.

Scenario	Hatch Date	Alteration in hatch date	Swim-up date	Alteration in swim-up date
Base-line	10 May	-	30 June	-
FullSpring	14 May	+ 4 Days	2 July	+ 2 Days
FullSummer	14 May	+ 4 Days	2 July	+ 2 Days
Dynamic2006	12 May	+ 2 Days	25 June	- 5 Days

Table 4.2. Ice formation potential for observed and simulated discharge scenarios.

	Base-line	A-FullSpring and B-FullSummer	Dynamic2006
No of events with ice potential	9	19	10
Latest event	4 January	24 February	24 February
Min. ice event [hours]	1.75	1	1.5
Max. ice event [hours]	86	103	19
Mean ice event [hours]	15	13	6
Median ice event [hours]	5	5	5
Sum [Days]	5.8	10.3	2.6
Change [Days]	-	+4.5	-3.2